Implication of stratospheric aerosol geoengineering on compound precipitation and temperature extremes in Africa

Salomon OBAHOUNDJE[1], Vami Herman NGUESSAN-BI[2], Arona DIEDHIOU[2,3], Ben KRAVITZ[4,5], John C. MOORE[6,7]

[1] LASMES - African Centre of Excellence on Climate Change, Biodiversity and Sustainable Agriculture / University Félix Houphouët Boigny, Abidjan, Côte d'Ivoire (obahoundjes@yahoo.com).

[2] CURAT (University Center of Applied Reseach in Remote Sensing) University Félix Houphouët-Boigny, 22 BP 801 Abidjan 22, Abidjan, Ivory Coast (vami@outlook.com).

[3] Univ. Grenoble Alpes, IRD, CNRS, Grenoble INP, IGE, F-38000 Grenoble, France (arona.diedhiou@ird.fr).

[4] Department of Earth and Atmospheric Sciences, Indiana University, Bloomington, IN, USA (bkravitz@iu.edu)

[5] Atmospheric Sciences and Global Change Division, Pacific Northwest National Laboratory, Richland, Washington, USA

[6] Arctic Centre, University of Lapland, Rovaniemi, Finland

[7] State Key Laboratory of Earth Surface Processes and Resource Ecology, College of Global Change and Earth System Science, Beijing Normal University, Beijing, China (john.moore.bnu@gmail.com)

Corresponding author address: arona.diedhiou@ird.fr

Abstract

Three Coupled Model Intercomparison Project 5 (CMIP5) models that simulated the G4 experiment of the Geoengineering Model Intercomparison Project (GeoMIP) were used to investigate the impact of stratospheric aerosol injection (SAI) on combined temperature and precipitation extremes in Africa that can have greater negative impacts on human and the environment than individual rainfall or temperature extremes. The examined compound extremes included the dry ($R_{warm|dry}$ and $R_{cold|dry}$) and wet ($R_{warm|wet}$ and $R_{cold|wet}$) modes assessed during the injection (SAI, 2050-2069) and post-injection (postSAI, 2070-2089) periods compared with the historical period (1986-2005). We found a significant projected change in the occurrence of both wet and dry modes during SAI and postSAI related to the historical period. The magnitude and sign of this change depend on the season and the geographical location. During the SAI and postSAI, the wet ($R_{warm|wet}$ and $R_{cold|wet}$) modes are projected to be significantly lower while the dry modes are noted to increase in a large part of African continent depending on the season and the geographical location and may consequently leads to an increase of the droughts prone areas. The termination effect is noted to reduce the occurrence of dry modes, which may reduce the potential negative effects of the injection after halting. As the effect may vary from one region to another and according to the season, it suggested assessing the key sector impacts of SAI. Thus, this change in dry modes due to SAI could affect all activities which depend on water resources such as water supply, agriculture and food production, energy demand, and production with adverse effects on health, security, and sustainable development, but this needs to be assessed and quantified at regional scales.

Keywords: GeoMIP, Compound extremes, Stratospheric aerosol injection, Injection effect, Termination effect

1. Introduction

To meet the Paris Agreement goal of keeping mean global rises below 1.5°C, mitigation measures to reduce greenhouse gases have been agreed upon at the state level in association with adaptation measures. Additionally, solar radiation management (SRM) technologies may play a potential future role in meeting the Paris Agreement (Nicholson *et al* 2018), although their impacts and the effects of terminating SRM are not yet well understood (Rabitz 2018). Much further research on SRM global-scale environmental, and social is required, while ethical and governance issues have been clearly stated. Continental- and local-scale studies on the implications of SRM are rare, especially in African subregions.

Stratospheric aerosol injection (SAI) is an untested geoengineering technique that creates an aerosol layer of aerosols, commonly assumed to be sulfuric acid and precursors in the stratosphere to scatter incoming solar radiation in the atmosphere. Indeed, SAI has recently received increased scientific attention (NASEM, 2021). The aim is to imitate the effects of explosive volcanic eruptions that are known to cool the planet (Budyko 1977, Crutzen 2006). The eruption of Mt. Pinatubo in 1991, which injected approximately 20 megatons of sulphur dioxide into the atmosphere cooled the planet and produced other climate impacts (Robock 2000; Rahm 2018). Although this idea seems to be a prominent domain, scientific knowledge of the probable impacts of the process on developing countries is rare. The effectiveness of SAI as well as its implications on temperature and precipitation extremes in African regions are nascent (Obahoundje *et al* 2022). Several existing studies are based on the Geoengineering Large Ensembles (GLENS) simulations, an extreme example of offsetting all climate change from Representative Concentration Pathway 8.5 (RCP8.5) from 2020 through 2100 (Tilmes et al., 2018). Under GLENS, over the African continent, SAI could significantly reduce temperature means and extremes (Pinto *et al* 2020). Over West Africa, the surface temperatures across a range of indices including cold days, cold nights, and cold spell duration during 2070-2090 would be effectively maintained to the current-day level (when compared to the control period, 2010–2030, RCP8.5) under the GLENS simulation (Alamou *et al* 2022). The effect on precipitation, however, is not as linear (Pinto *et al* 2020). Precipitation is projected to increase by 45%, 20%, and 5% during the monsoon period in the Northern Sahel, Southern Sahel, and Western Africa regions, respectively, under RCP8.5. Under GLENS simulations, by comparing 2050–2069 relative to the current climate (2010–2029 with RCP8.5), West African summer monsoon (during July August September-October) rainfall is virtually unchanged in the Northern Sahel region but declines by 4% (0.19± 0.22 mm) and 11% (0.72 ±0.27 mm) in the Southern Sahel and Western Africa regions, respectively (Da-Allada *et al* 2020). In the far future (2070–2090), GLENS reveals a significant increase in the total annual and extremes precipitation but the magnitude of change may vary according to the geographical location of each sub region of the West Africa (Alamou *et al* 2022). These changes in extreme precipitation indices are associated with changes in the Atlantic Multidecadal Oscillation, NINO3.4 (average SST anomalies in the NINO3.4 region over 5°N to 5°S, from 170°W to 120°W), and the Indian Ocean Dipole, and driven by changes in near-surface specific humidity and atmospheric circulation (Alamou *et al* 2022). Overall, the GLENS simulations may affect all processes involved in precipitation mechanism (Karami *et al* 2020). Geoengineering could offset the projected end-of-century risk of 'Day Zero' level droughts by approximately 90%, keeping the risk of such drought similar to the risk in Cape Town, South Africa today (Odoulami *et al* 2020).

Most the studies of the Stratospheric Aerosol Geoengineering impacts over Africa made the use of GLENS, but few s focuses on the implication of Geoengineering Model Intercomparison Project (GeoMIP) especially its forth standardized simulation G4 involving increased amounts of stratospheric sulfate aerosols or SAI. Specifically, the implications of SAI on climate extreme events and compound extremes in African subregions are not known.

Moreover, the difference between SAI-based climate simulations performed with the GeoMIP and Phase 5 of the Coupled Model Intercomparison Project (CMIP5) is not well known in Africa.

Availability and accessibility of daily meteorological data are limited, hence assessing the occurrence of and variability in extreme events at continental, regional, national, and local scales is complex. To overcome this obstacle, the evolution of extreme climate events over the regions is characterized using models or reanalysis products. Climate extreme events such as floods and droughts have become common in Africa (Leonard *et al* 2014) and are responsible for many of the most severe weather-related and climate-related impacts experienced on the continent (Zscheischler *et al* 2020). For instance, the observed climate extreme events including flooding and drought in West Africa during the last 30 years can be explained by the fact that the rainfall events have become less frequent but more intense along the coast of the Gulf of Guinea while the Sahel part has become wetter associated with shorter and frequent dry spells (Bichet and Diedhiou 2018a, 2018b). An increase in the co-occurrence of extreme weather events can have many negative effects on society in African countries wherein the populations are largely dependent on rainfed agriculture (over 95% of African food production is rainfed, according to Abrams (2018)) and hydroelectricity (Falchetta *et al* 2019).

Compound precipitation and temperature extremes, which are also known as simultaneous or coincident extremes, contribute to societal and environmental risks. These concomitant events can have greater negative effects on human health and the environment than individual rainfall or temperature extremes (Leonard *et al* 2014). Compound extremes are categorized into four groups depending on the characteristics of their occurrence, namely, preconditioned, multivariate, temporally compounding, and spatially compounding events (Zscheischler *et al* 2020). In the past, the occurrence of compound warm spells and droughts in the

Mediterranean Basin, including northern Africa, has been noted to have increased significantly (Vogel *et al* 2021), while compound drought and extreme heat events have increased in large areas of Europe, namely, in parts of Western Europe, Italy, the Balkan Peninsula, and Northern and Eastern Europe (Bezak and Mikoš 2020) as well as in China (Yu and Zhai 2020) and the USA (Alizadeh *et al* 2020). These trends have attracted scientific interest. Thus, studies on projected compound climate extremes are increasing worldwide (Aghakouchak *et al.*, 2020; Leonard et al., 2014; Seneviratne *et al.*, 2012), especially in China (Zhan *et al* 2020, Zhou and Liu 2018, Lu *et al* 2018, Chen *et al* 2019, Zhang *et al* 2018, Hao *et al* 2018b), the USA (Tavakol *et al* 2020) and Africa (Weber *et al* 2020, Diba *et al* 2021), due to the large impacts these extreme events have on humans and ecosystems. Changes in the severity of compound drought and hot extreme events have been projected for global land areas (Hao *et al.*, 2018; Sedlmeier *et al.*, 2018; Wu *et al.*, 2021). For instance, climate model projections under RCP8.5 scenario show that the global land (Hao *et al* 2018a) and cropland areas affected by compound dry and hot events will increase by 1.7-1.8 times by the end of the twenty-first century (Wu *et al* 2020). In 2050-2099, the spatial extent of global land areas affected by dry and hot compounds during the June-July-August (December-January-February) season will increase by 12.38-17.20 % (7.83-11.19 %) compared to 1950-1999, while the spatial extent of global cropland areas affected by the same events will increase by 14.69-19.63 % (9.60-14.48 %) (Wu *et al* 2020). Combinations of temperature (cold or warm) and precipitation (wet or dry) extremes have indicated that the frequency of cold modes (cold|dry and cold|wet) will significantly decrease (Beniston 2009) while warm modes (warm|dry and warm|wet) mode will sharply increase in the 21st century in Europe (Sedlmeier *et al* 2018). Climate extremes co-occurrence expose increasingly large populations to the devastating effects of repeat, chronic, and sequential natural disasters (Drakes and Tate 2022).

Generally, there is little literature addressing the climate extremes compound in Africa. The existing studies have mainly focused on extremes based on a single variable, such as intense/low precipitation, maximum/minimum temperatures (Diba *et al* 2021), or the exposure risk of continents to the occurrence of heatwaves, droughts, and intense rainfall events (Diedhiou *et al* 2018); however, less attention has been given to the co-occurrence of these extremes (Weber *et al* 2020). There is a lack of understanding of the compound impacts resulting from concomitant temperature and precipitation stress in Africa (Niang *et al* 2014). Therefore, a better understanding of compound events could help policymakers, local populations, and scientists develop strategies and adaptation measures (Zscheischler *et al* 2018). Weber *et al.* (2020) found that all addressed compound climate extremes are projected to increase in frequency, and the changes will be greater under scenarios with more warming. Weber *et al.* (2020) also highlighted that the population exposure will be greater under RCP8.5 than under RCP2.6 and that West Africa, Central-East Africa, and Northeast and Southeast Africa are most at risk. Changes in the occurrence of climate compound extremes have been found to impact hydrological systems (Hao *et al.*, 2018) increased wildfire risks, water availability, human mortality, energy demand and supplies, crop production, food security, and flash flooding (Weber *et al* 2020). Diba *et al.* (2021) predicted the strong occurrence of the extreme wet/warm mode over West-central and southern Senegal and an increase in the dry/warm mode over northwest, central-west, and southwest Senegal in the future. The wet/warm mode will decrease over north-western, central, and southern Senegal in the near future and over the whole country of Senegal in the far future. Compound extremes exhibit large spatial variability in Africa motivating investigation in each African subregion based on the CMIP5 experiments as well as GeoMIP simulations of SAI. We explore the projected implication of SRM technology on the occurrence of the four compound extreme modes. Specifically differences between the GeoMIP G4 SAI experiment and the modest greenhouse gas emission RCP4.5 scenario experiments in the occurrence of climate (temperature and precipitation) compound extremes. Additionally, we consider the termination effects of SAI on climate compound extremes in Africa. This study aims (i) to evaluate the changes in extreme compounds of precipitation and temperature-induced by SAI under G4 and RCP4.5 simulations during the deployment of SAI, (ii) to determine the effects of SAI cessation, and (iii) to assess the regional implications of SAI during the different seasons.

2. Data and Methodology

The extreme compounds of temperature and precipitation were computed from three Earth System Models (ESM) that simulated the GeoMIP experiment G4 (Kravitz *et al* 2011). This experiment involves daily injections of SO_2 at a rate of 5 Tg yr^{-1} into the equatorial lower stratosphere (~16–25 km in altitude) from 2020 to 2069 while the representative concentration pathway (RCP) 4.5 scenario defines greenhouse gas (GHG) emissions (Fig 1). The SAI stops in 2069, but the experiment continues for an additional 20 years to 2089 with only GHG forcing, as specified by RCP4.5 (Kravitz *et al* 2011). We used MIROC-ESM (Watanabe *et al* 2011), MIROC-ESM-CHEM (Watanabe *et al* 2011), and CanESM2 (Arora *et al* 2011) ESM all with an atmospheric resolution of 2.81°. These models were chosen based on the completeness of the data for all considered variables and chosen periods.

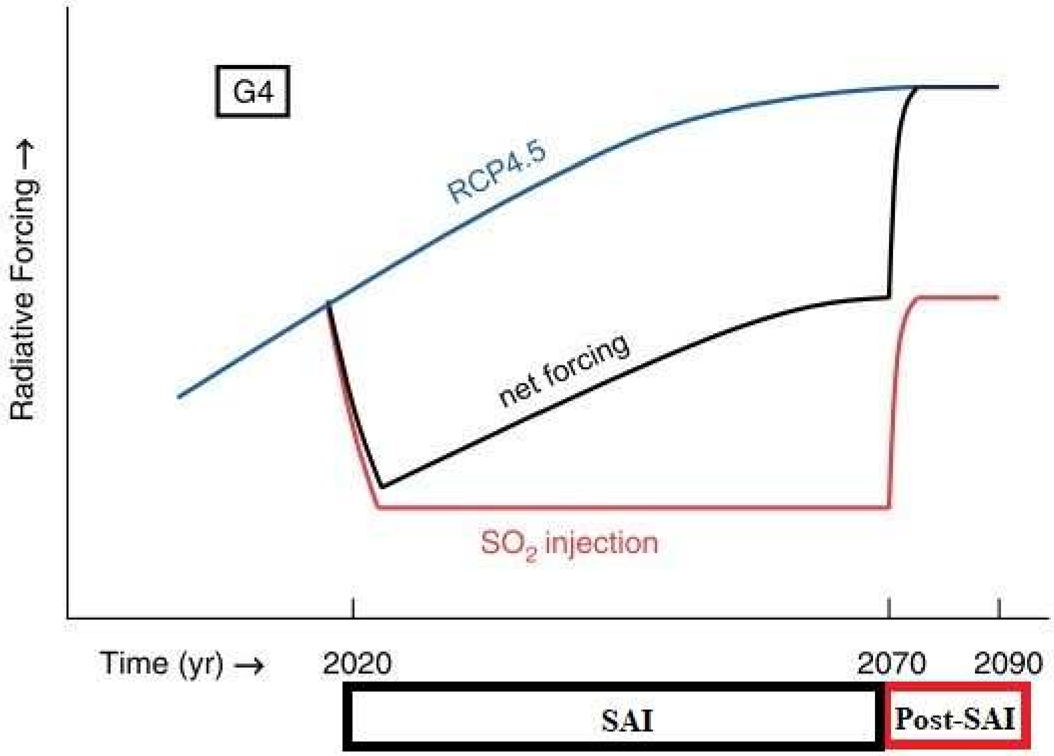

Figure 1. Schematic of the G4 experiments adapted from Kravitz et al. (2011). This experiment was based on the RCP4.5 scenario, wherein immediate negative radiative forcing is produced by an injection of SO_2 into the tropical lower stratosphere at a rate of 5 Tg per year.

The changes in compound extremes during the injection (2050-2069) and post-injection (2070-2089) periods relative to the historical period (1986-2005) were assessed on the 3-monthly (seasonal) scale. The future change was computed as the difference between the mean over the future period (two separate periods: the injection and post-injection periods) and the historical period. The defined seasons are December-January-February (DJF), March-April-May (MAM), June-July-August (JJA), and September-October-November (SON). To capture the dominant effects of SAI, the G4 simulations were compared to RCP4.5 during the injection period as well as the post-injection period. The termination effect was computed by comparing the mean values over the injection period to the post-injection effects when SAI was abruptly terminated.

A *Student's t* test was used to evaluate the significance of the mean differences between the two simulations (G4 and RCP4.5) and periods. The advantages of *Student's t* test compared to non-parametric tests for such applications are described by Lydersen (2015). The details of its computation can be found in Janssen (2005). For the analyses presented here over 20 years (2050-2069 for changes during the SAI period) and 20 years (2070-2089 for changes during the post-injection period), statistically significant values are defined at the 95% confidence level.

The different African subregions that we evaluated in this study are presented in Fig 2, and their geographical boundaries are summarized in Table 2. These subregions are consistent with those identified in the IPCC SREX (e.g., Giorgi and Francisco 2000; Seneviratne et al. 2012).

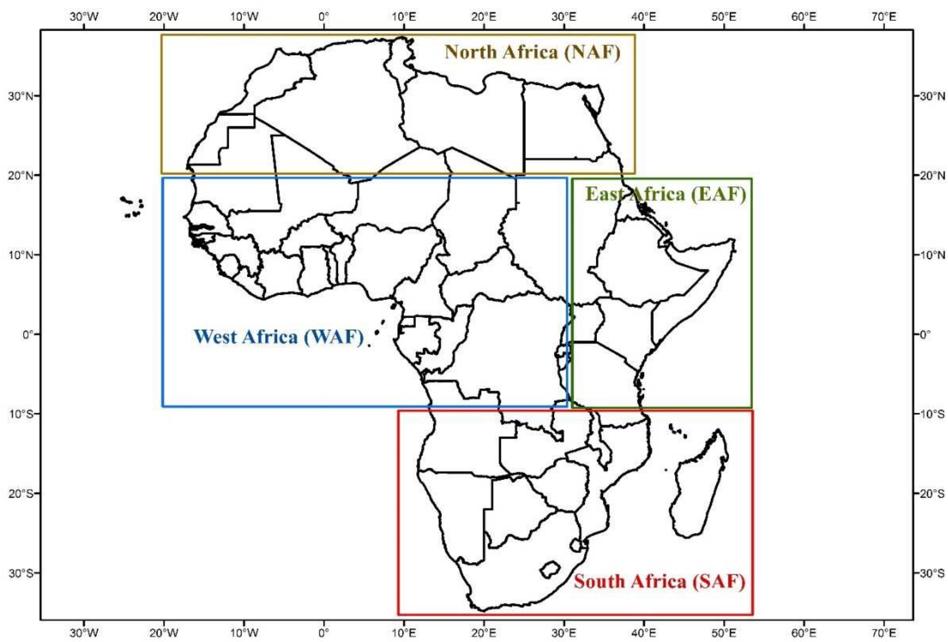

Figure 2. Map of African countries in different subregions.

Table 2: Definitions of the African subregions used for this study.

Region	Longitude	Latitude
East Africa (EAF)	30° – 52°E	10°S – 20°N
North Africa (NAF)	18°W – 40°E	20° – 38°N
South Africa (SAF)	10° – 52°E	10° – 36°S
West Africa (WAF)	18°W – 30°E	10°S – 20°N

We computed the extreme indices of precipitation (dry and wet) and temperature (warm and cold) according to the World Meteorological Organization (WMO) guidelines (Klein Tank *et al* 2009). A compound extreme event may be defined as two or more extreme events occurring simultaneously or sequentially or a combination of events that are not themselves extremes but lead to an extreme event or impact when combined (Seneviratne *et al* 2012).

A wet day is with precipitation above the 90th percentile of seasonally averaged daily precipitation, while a dry day is with precipitation below the 10^{th} percentile. A cold day refers to a day with a temperature below the 10th percentile of seasonally averaged minimum daily temperatures, while a warm day corresponds to a day with a temperature above the 90^{th} percentile of maximum seasonally averaged daily temperatures. When an extreme precipitation condition (wet/dry) occurs simultaneously with a temperature extreme (warm/cold), it results in a compound extreme. Here, we give particular attention to four compound extremes modes: the $R_{warm|dry}$, $R_{warm|wet}$, $R_{cold|dry}$, and $R_{cold|wet}$ modes that have been widely used to investigate climate extremes at the regional scale (Diba *et al* 2021), continental-scale (Weber *et al* 2020), and global scale(Leonard *et al.*, 2014; Seneviratne *et al.*, 2012). The number of days of the occurrence of these defined extremes was computed for each season and experiment. Then, they were averaged over each season and each experiment before the assessment of the implication of injection and termination.

We use four compound extremes namely warm|dry($R_{warm|dry}$), cold|dry ($R_{cold|dry}$), warm|wet ($R_{warm|wet}$), and cold|wet ($R_{cold|wet}$). The $R_{warm|dry}$ refers to the total number of days with daily precipitation below the 10th percentile of average daily precipitation and days with daily temperatures above the 90th percentile of maximum daily temperatures. The $R_{cold|dry}$ stands for the total number of days with daily precipitation below the 10th percentile of average daily precipitation and days with daily temperatures below the 10th percentile of minimum daily temperatures. $R_{warm|wet}$ is defined as the total number of days with daily precipitation above the 90th percentile of average daily precipitation and days with daily temperatures above the 90th percentile of maximum daily temperatures. Lastly, $R_{cold|wet}$ refers to the total number of days with daily precipitation above the 90th percentile of average daily precipitation and days with daily temperatures below the 10th percentile of minimum daily temperatures. To enable the extraction of a relatively large number of compound events for this study, we define dry conditions using the below 50th percentile of daily precipitation and wet conditions using the above 50th percentile of daily precipitation as a threshold base on a previous study (Feng *et al* 2020). The temperature thresholds are kept to 10th percentile of daily minimum temperature for cold conditions and 90th percentile of the daily maximum temperature for warm conditions (Feng *et al* 2020).

3. Results

3.1. Changes in the occurrence of dry compound modes

The change in the occurrence of compound modes during and after injection related to the historical period is presented in Appendix A (FigA.1-4) according to the season. By comparing G4 (SAI and postSAI) to the historical period (1986-2005, See FigA.1 in appendix), the $R_{warm|dry}$ shows a significant increase in large parts of the continent during all seasons except the Sahelian band during DJF and SON and western part of NAF and south-eastern part of EAF during injection (G4 over 2030–2069 compared to historical run 1986-2005; see FigA.1 b for all seasons). There is no significant change after SAI stoppage (G4 over 2070–2089 compared to historical run 1986-2005; see FigA.1 d for all seasons in appendix). $R_{cold|dry}$ shows a significant decrease in large parts of the continent during DJF, JJA, and SON while a significant increase is noted during MAM except over the Sahelian band during injection (G4 over 2030–2069 compared to historical run 1986-2005; see FigA.2 b for all seasons). There is no significant change after SAI stoppage (G4 over 2070–2089 compared to historical run 1986-2005; see FigA.2 d for all seasons).

Fig 3 presents the changes in the total number of days with daily precipitation below the 50th percentile of average daily precipitation and days with daily temperatures above the 90th percentile of maximum daily temperatures ($R_{warm|dry}$) for DJF (Fig 3a-c), MAM (Fig 3d-f), JJA (Fig 3g-i) and SON (Fig 3j-l).

During the injection period, the occurrence of the $R_{warm|dry}$ mode compound extreme is simulated to be lower in G4 than in RCP4.5 over the NAF and Sahelian bands of WAF and EAF subregions during DJF (Fig 3a) while significantly greater over the tropical band for the remain seasons MAM, JJA, SON (Fig 3d,g,j). The spatial distribution depends on the season. However, the termination of SAI (2070-2089, compared to the 2050-2069 period in G4) is noted to lead to a significant decrease in the occurrence of the $R_{warm|dry}$ mode over the whole continent for all seasons (Fig3b,e,h,k) except the Sahelian band during DJF and SON seasons (Fig 3b,k). The occurrence of the $R_{warm|dry}$ mode due to the termination effect in G4 will be greater than that in RCP4.5 in large parts of the African continent during all seasons DJF, MAM, JJA, SON (Fig 3c, f, i, l).

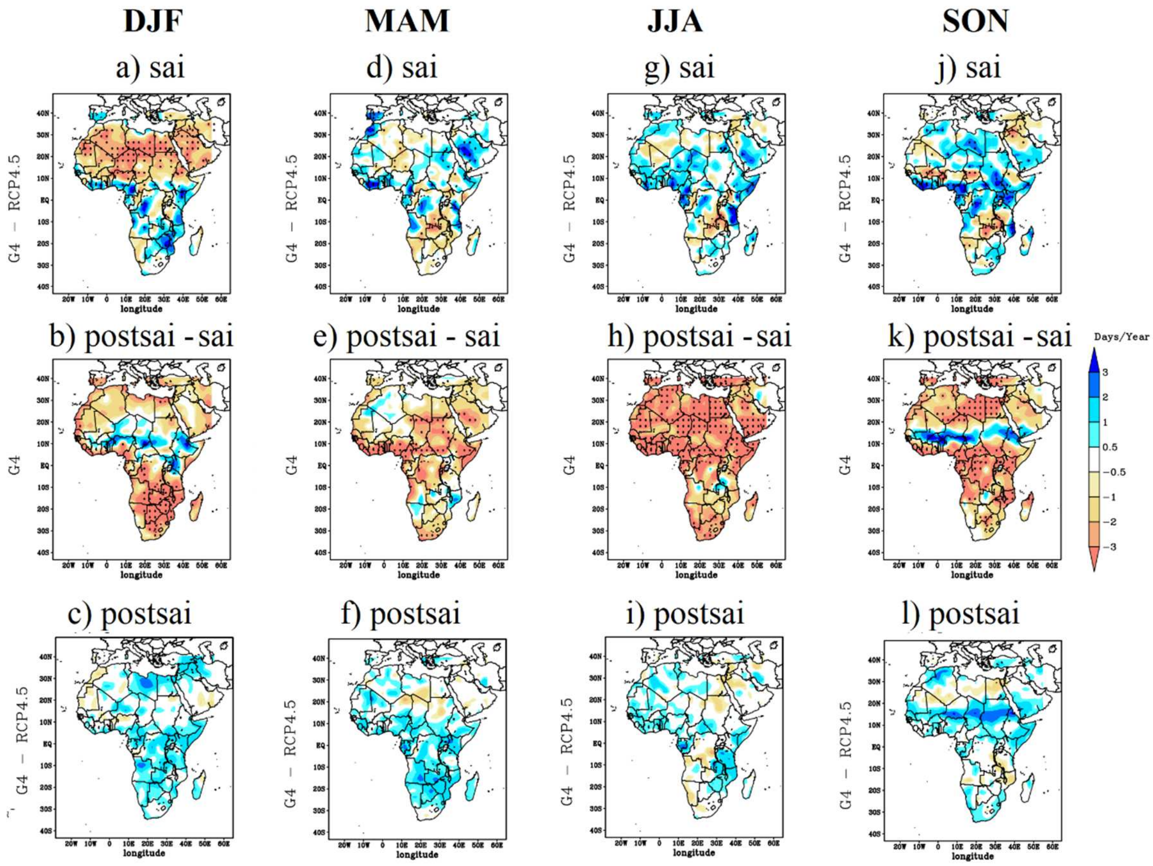

Figure 3. Three model ensemble mean changes in warm-dry compound extreme events in different seasons: DJF (first column), MAM (second column), JJA (third column) and SON (fourth column). NB: The black dots on the maps delimit areas with significant changes at the 95% confidence level; the SAI period refers to 2050-2069 and the postSAI period refers to 2070-2089. The first row of figures (3a, 3d, 3g and 3j) compares the G4 to RCP4.5 experiments during the injection period (SAI, 2050-2069). The second row of figures (3b, 3e, 3h and 3k) shows the termination effect by comparing changes between the post-injection period (postSAI or 2070-2089) and the injection period (SAI or 2050-2069) in the G4 experiment. Last, the third row of figures (3c, 3f, 3i and 3l) compares the changes between G4 and RCP4.5 during the post-injection (postSAI) period.

Fig 4 presents the changes in the occurrence of the total number of days with daily precipitation below the 50th percentile of the average daily precipitation and days with daily temperatures below the 10th percentile of minimum daily temperatures (the $R_{cold|dry}$ mode). The $R_{cold|dry}$ mode is presented according to the season, namely, DJF (Fig 4a-c), MAM (Fig 4d-f), JJA (Fig 4g-i) and SON (Fig 4j-l).

During the injection period, the occurrence of the $R_{cold|dry}$ mode compound extreme is simulated to be greater in G4 than in RCP4.5 over the whole African continent (with significantly greater occurrences in some subregions during some seasons) except in the central of SAF during MAM, Sahelian band and Gulf of Guinean during JJA (Fig 4a, d, g, j). The spatial distribution depends on the season (Fig 4a, d, g, j). However, the termination of SAI (2070-2089, compared to the 2050-2069 period in G4) is noted to lead to a significant increase in the occurrence of the $R_{cold|dry}$ mode over the whole continent for all seasons except over NAF and northern of WAF and EAF during MAM, and northern of NAF during JJA (Fig 4b, e, h,k)). The occurrence of the $R_{cold|dry}$ mode due to the termination effect in G4 will be greater than that in RCP4.5 in large parts of the African continent during DJF, JJA, and SON (Fig 4c, i, l).

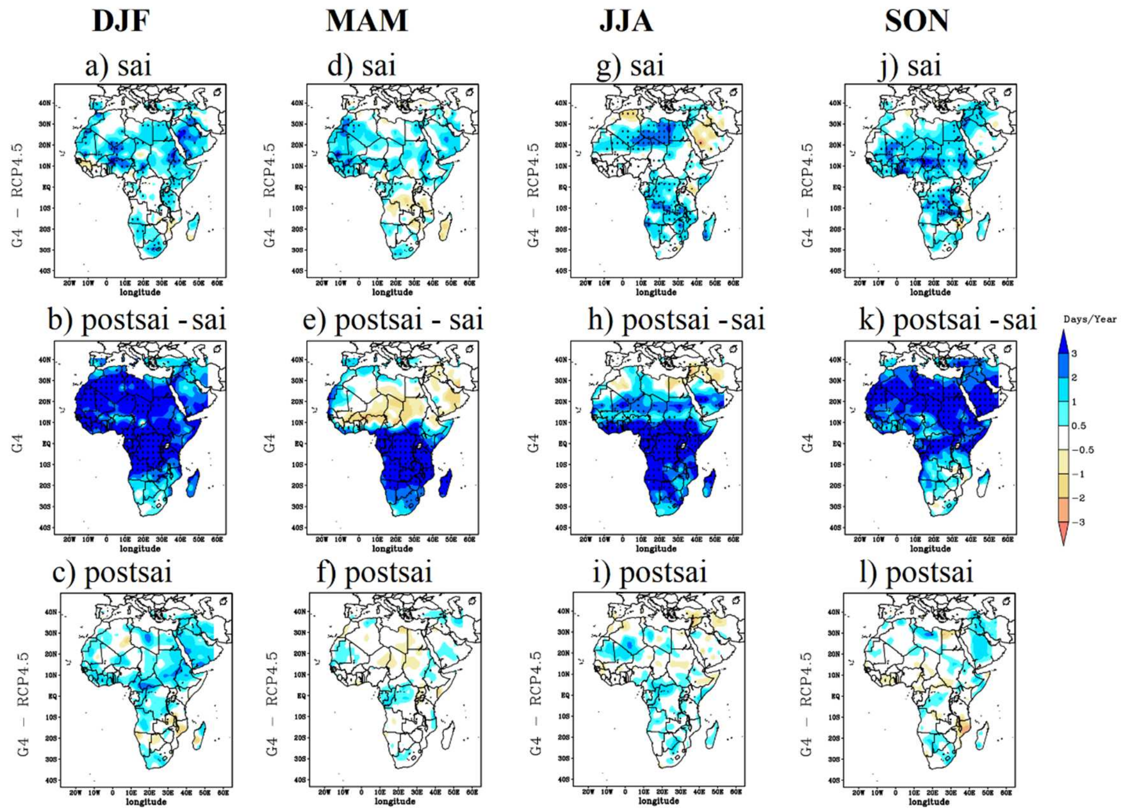

Figure 4. Three model ensemble mean changes in $R_{cold|dry}$ compound extreme events in different seasons: DJF (first column), MAM (second column), JJA (third column) and SON (fourth column). NB: The black dots on the maps delimit areas with significant changes at the 95% confidence level; the SAI period refers to 2050-2069, and the postSAI period refers to 2070-2089. The first row of figures (4a, 4d, 4g and 4j) compares the G4 experiment to RCP4.5 during the injection period (SAI, 2050-2069). The second row of figures (4b, 4e, 4h and 4k) shows the termination effect by comparing the changes between the post-injection period (postSAI or 2070-2089) and the injection period (SAI or 2050-2069) in the G4 experiment. Last, the third row of figures (4c, 4f, 4i, and 4l) compares the changes between G4 and RCP4.5 during the post-injection period (postSAI).

3.2. Change in the occurrence of the compound wet modes

When comparing G4 (ASI and postSAI) to the historical period (1986-2005, See FigA.3b in of all seasons in appendix), the $R_{warm|wet}$ is noted to decrease significantly during DJF(over the Sahelian band and NAF), MAM(Sahelian band and eastern NAF), JJA(SAF) and SON (SAF associated with a significant increase over NAF) during the injection. The termination effect may lead to a significant decrease in the occurrence of $R_{warm|wet}$ events in some parts of the continent depending on the season (See FigA.3 d of all seasons). By comparing G4 (ASI and postSAI) to the historical period (1986-2005, See FigA.4b in of all seasons in appendix), the $R_{cold|wet}$ is noted to decrease significantly over extratropical bands (SAF and NAF) and tropical bands (WAF and EAF) during JJA and SON during the injection. The termination effect may significantly increase the occurrence of $R_{cold|wet}$ events over SAF during DJF and over WAF and some parts of SAF and NAF during JJA (See FigA.4d of all seasons).

Fig 5 presents the changes in the occurrence of the total number of days with daily precipitation above the 50^{th} percentile of average daily precipitation and days with daily temperatures above the 90^{th} percentile of maximum daily temperatures (the $R_{warm|wet}$ mode). The $R_{warm|wet}$ mode is presented according to the season, namely, DJF (Fig 5a-c), MAM (Fig 5d-f), JJA (Fig 5g-i) and SON (Fig 5j-l).

During the injection period, the occurrence of the $R_{warm|wet}$ mode compound extreme is simulated to be significantly lessened in G4 than in RCP4.5 over the whole African continent (except WAF and NAF during DJF and NAF during the rest of the seasons) (Fig 5a, d, g, j). However, the termination of SAI (2070-2089, compared to the 2050-2069 period in G4) is noted to lead to a lower (significant over tropical band during DJF) occurrence of the $R_{warm|wet}$ mode over the tropical band (WAF and SAF during DJF) and extratropical (SAF during MAM (Fig 5b, e). During the JJA and SON seasons, a significant decrease is noted over large parts of the continent (Fig 5h,k). The occurrence of the $R_{warm|wet}$ mode due to the termination effect in G4 will be lower (not significant) than that in RCP4.5 in large parts of the African continent during all seasons (Fig 5c, f, i, l).

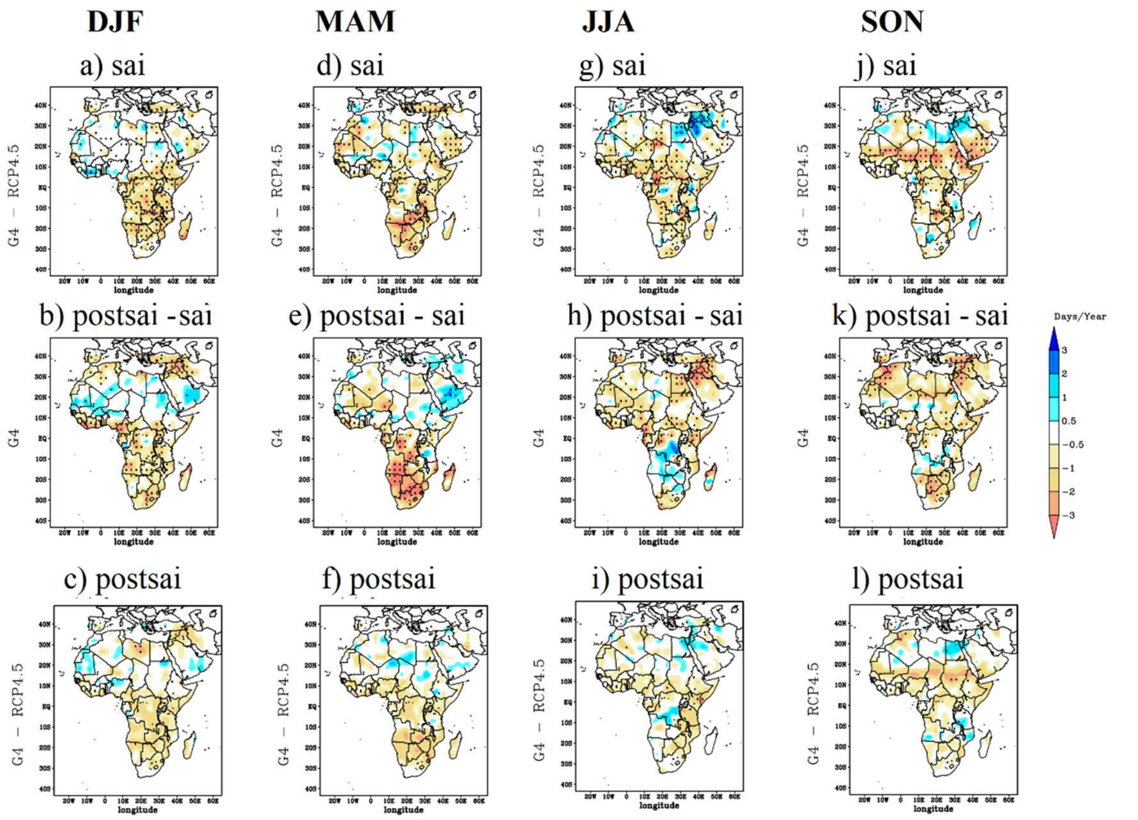

Figure 5. Same as Figure 3 but for warm-wet compound extreme events

Fig 6 presents the changes in the occurrence of the total number of days with daily precipitation above the 50th percentile of average daily precipitation and days with daily temperatures below the 10th percentile of maximum daily temperatures (the $R_{cold|wet}$ mode). The $R_{cold|wet}$ mode is presented according to the season, namely, DJF (Fig 6a-c), MAM (Fig 6d-f), JJA (Fig 6g-i), and SON (Fig 6j-l).

During the injection and after the stoppage of SAI, there is no change in the occurrence of the $R_{cold|wet}$ mode compound extreme between G4 and in RCP4.5 (Fig.6.a, d, g, j, c, f, i, l). However, the termination of SAI (2070-2089, compared to the 2050-2069 period in G4) is noted to lead to a significant increase in the occurrence of the $R_{warm|wet}$ model over extratropical bands (western Sahel in WAF and western of NAF, SAF during DJF, southern of SAF, Gulf of Guinean of WAF, southern of EAF during MAM, entire continent during JJA and Gulf of Guinea, Central Africa and EAF tropical during SON) (Fig 6b, e, h, k).

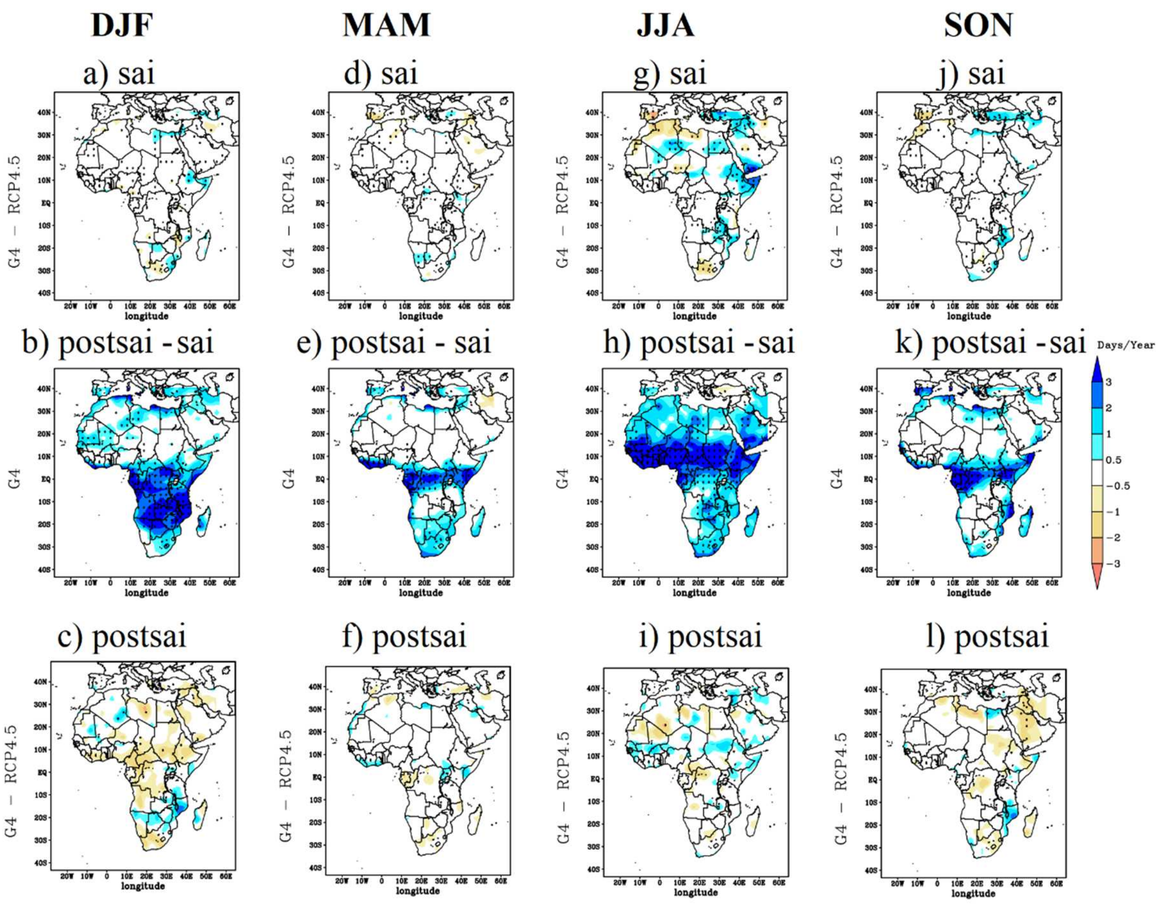

Figure 6. Same as Figure 4 but for cold-wet compound extreme events

4. Discussion

The frequencies of compound climate extremes have increased over the past seven decades (He and Sheffield 2020), especially warm modes (Alizadeh *et al.*, 2020; Bezak & Mikoš, 2020; Vogel *et al.*, 2021; Yu & Zhai, 2020), and these frequencies may be further amplified in the future (Wu *et al* 2020). Tencer *et al.* (2016) related these increases in compound climate extremes to changes in land-ocean-atmosphere processes due to changes in ocean and land temperatures.

During SAI, $R_{warm|dry}$ shows a significant decrease in large parts of the continent during DJF and in some parts of the continent for the rest of the seasons. The reduction in $R_{warm|dry}$ in large parts of Africa shows the effectiveness of SAI because this mode is projected to increase (Uğuz *et al* 2020)(Zhang *et al* 2022) due to global warming. The $R_{cold|dry}$ shows a significant increase in large parts of the continent during DJF, MAM and SON associated with a significant decrease during JJA over the western Sahel and western NAF during injection and after stoppage. The $R_{warm|wet}$ shows a significant reduction in most parts of the continent during the injection. This suggests the effectiveness of SAI will in return cools down the continental surface temperature but increases the number of co-occurrence of dry events.

Some existing global-scale studies (Aghakouchak *et al.*, 2020; Wu *et al.*, 2020) performed in Europe (Sedlmeier *et al.*, 2018) and Africa (Weber *et al* 2020) found that all compound climate extremes related to the warming mode will increase in frequency depending on the GHG scenario. Under the RCP8.5 scenario global land and crop areas affected by compound dry and warm events increase by 1.7-1.8 times by the end of the 21st century (Wu et al., 2020). Weber *et al.* (2020) showed that the projected increase in the occurrence of compound climate extremes due to the warm mode will increase the vulnerability of the population compared to the present day, and this exposure may vary according to region. Regions such as West Africa, Central-East Africa, and Northeast and Southeast Africa may be most exposed to the climate extremes compound effect.

The analysis performed in the current study reveals that the dry modes ($R_{warm|dry}$ and $R_{cold|dry}$) show a significant increase (G4 compared to RCP4.5) in large parts of the continent during all seasons while the termination effect may lead to the reduction of the frequencies of

$R_{warm|dry}$ and increase in co-occurrence $R_{cold|dry}$. A significantly reduction in the co-occurrence of wet modes ($R_{cold|wet}$ and $R_{warm|wet}$) is noted in large part of the continent during SAI and postSAI (G4 compared to RCP4.5) while the termination effect will likely increase the $R_{cold|wet}$ and reduce the $R_{warm|we}$ (postSAI compared to SAI). The spatial distribution of the difference in the occurrence of dry modes according to the seasons suggests that the movement of the ITCZ controls these. This is consistent with the well-known globally lowered precipitation and humidity expected under SAI (Bala *et al* 2008) inducing more dry events rather than wet events in Africa. These projected changes in the occurrence of compound climate extremes may increase the vulnerability of the African population to changing climatic conditions, which are already challenging to adapt to and mitigate.

Some regions of the world where climate extremes compound were found experience some negative effects. For instance, during the 1999-2002 and 2009-2010 periods, Mongolian countries experienced two types of compound climate extremes, namely $R_{warm|dry}$ events during summer and $R_{cold|wet}$ events during winter; these extreme events led to increased poverty and mass migration from rural to urban areas and from remote to central regions (Field *et al* 2011). The occurrence of $R_{warm|dry}$ events leads to a lack of pastureland for livestock, which is the main economic activity in Mongolia. In China, an increase in observed compound hots events was noted caused by anthropogenic factors (Wang *et al* 2022). Indeed, compound dry and hot events are becoming more common as a result of anthropogenic forcing at the global and continental scales (Zhang *et al* 2022). In Africa, the projected increase in dry modes ($R_{warm|dry}$ and $R_{cold|dry}$) associated with a reduction of wet modes ($R_{warm|wet}$ and $R_{cold|wet}$) may also lead to droughts, disrupt food and water supplies and consequently provoke health issues, as shown by Hales *et al.*, (2003). Additionally, this may intensify the drought-prone areas and increase the dry spells which have become more frequent in the Guinea zone (Bichet and Diedhiou 2018a) and Sahelian band (Bichet and Diedhiou 2018b) of WAF. Consequently, these may affect economic factors through population displacements, housing/urbanization/population density impacts, and public health infrastructure impacts and become new transboundary conflictual sources (Brown and Crawford 2008). Moreover, social factors could be affected by human behavior (water storage practices), land use (irrigation/forest clearance/livestock), herd immunity, and nutritional status. Furthermore, the abundance and distribution behaviors of ecological vectors and pathogens will change due to the increase in the co-occurrence of temperature and precipitation extremes. The occurrence of the climate extremes compound (increase dry modes associated with decrease in wet modes) could affect the energy demand, production (especially hydropower) and distribution factors. Nevertheless, the termination effect is noted to reduce dry modes ($R_{warm|dry}$ and $R_{cold|dry}$) and $R_{warm|wet}$ during DJF and MAM with increase during JJA and SON while $R_{cold|wet}$ could increase during DJF(Western Sahel and NAF), MAM (SAF), JJA (NAF and WAF) and SON(SAF, southern of WAF and EAF). This means that after halting the injection, the risk of drought could be reduced but exposed the WAF and NAF regions to the risk of flooding during JJA and SON.

5. Conclusion

Studies on the incidence of compound temperature and precipitation extreme indices in Africa in the future are few, and knowledge of the implications of solar radiation management technologies for these compound extremes is scarce. This paper analyses the changes in the implications of four different compounds based on dry ($R_{warm|dry}$ and $R_{cold|dry}$) and wet ($R_{warm|wet}$ and $R_{cold|wet}$) modes using two different simulations. The first simulation is based on the SAI of the G4 experiment GeoMIP, while the second simulation is based on the RCP4.5 experiment of the CMIP5 simulation. Three ESM and their ensemble mean simulations of RCP4.5 (CMIP5) and G4 (GeoMIP) experiments were used to investigate the impact of SAI and its termination on the temperature and precipitation compound extremes in four subregions of Africa. The analysis was based on the injection (SAI, 2050-2069) and termination (post-injection, 2070-2089) periods. We found that the occurrence of dry modes ($R_{warm|dry}$ and $R_{cold|dry}$) will increase (G4 compared to the RCP4.5 experiment) while a decrease is noted for the wet modes ($R_{cold|wet}$ and $R_{warm|wet}$) during all seasons (DJF, MAM, JJA, and SON) during SAI and postSAI. But the magnitude of change varies seasonally and according to the geographical location related to the movement of the ITCZ position. This change in the occurrence of dry and wet modes could negatively affect all the activities sectors from agriculture to food, water resources, energy demand and production, health, security, socioeconomic, and politic. Nevertheless, the termination may reduce the negative effects.

A deeper analysis of the implications of the G4 experiment concerning other SAI as well as different SRM schemes using regional climate models or with advanced statistical methods would elucidate the African subregional responses. Additionally, bias correcting the model compound extreme incidences outputs with the available observational datasets, proxy, or remotely sensed products would improve the reliability of SRM impacts on the hydrological cycle, water resource availability, agriculture, and energy production. Since rain-fed agriculture makes up a huge fraction of African economies, such investigations would be a basic requirement to understand the impacts of compound temperature and precipitation extremes resulting from SAI geoengineering.

Acknowledgment: The research undertaken by the Côte d'Ivoire team in Africa and leading to this publication has received the financial support of the DECIMALS fund of the Solar Radiation Management Governance Initiative, set up by the Royal Society, Environmental Defense Fund, and The World Academy of Sciences (TWAS) and funded by the Open Philanthropy Project. This research on the impact of SRM in Africa is co-funded by IRD (Institut de Recherche pour le Développement; France) grant number UMR IGE Imputation

252RA5. The GEOMIP data used in this study are open data available via the Earth System Grid. Support for B.K. was provided in part by the National Science Foundation through agreement CBET-1931641, the Indiana University Environmental Resilience Institute, and the *Prepared for Environmental Change* Grand Challenge initiative.

References

Abrams L 2018 *Unlocking the potential of enhanced rainfed agriculture. Report no. 39* (Stockholm) Online: https://www.siwi.org/wp-content/uploads/2018/12/Unlocking-the-potential-of-rainfed-agriculture-2018-FINAL.pdf

Aghakouchak A, Chiang F, Huning L S, Love C A, Mallakpour I, Mazdiyasni O, Moftakhari H, Papalexiou S M, Ragno E and Sadegh M 2020 Climate Extremes and Compound Hazards in a Warming World *Annu. Rev. Earth Planet. Sci.* **48** 519–48

Alamou E A, Zandagba J E, Biao E I, Obada E, Da-Allada C Y, Bonou F K, Pomalegni Y, Baloitcha E, Tilmes S and Irvine P J 2022 Impact of Stratospheric Aerosol Geoengineering on Extreme Precipitation and Temperature Indices in West Africa Using GLENS Simulations *J. Geophys. Res. Atmos.* **127** 1–20

Alizadeh M R, Adamowski J, Nikoo M R, AghaKouchak A, Dennison P and Sadegh M 2020 A century of observations reveals increasing likelihood of continental-scale compound dry-hot extremes *Sci. Adv.* **6** 1–12

Arora V K, Scinocca J F, Boer G J, Christian J R, Denman K L, Flato G M, Kharin V V., Lee W G and Merryfield W J 2011 Carbon emission limits required to satisfy future representative concentration pathways of greenhouse gases *Geophys. Res. Lett.* **38** 3–8

Bala G, Duffy P B and Taylor K E 2008 Impact of geoengineering schemes on the global hydrological cycle *Proc. Natl. Acad. Sci. U. S. A.* **105** 7664–9

Beniston M 2009 Trends in joint quantiles of temperature and precipitation in Europe since 1901 and projected for 2100 *Geophys. Res. Lett.* **36** 1–6

Bezak N and Mikoš M 2020 Changes in the compound drought and extreme heat occurrence in the 1961–2018 period at the european scale *Water (Switzerland)* **12**

Bichet A and Diedhiou A 2018a Less frequent and more intense rainfall along the coast of the Gulf of Guinea in West and Central Africa (1981 – 2014) *Clim. Res. (Clim Res)* **76** 191–201

Bichet A and Diedhiou A 2018b West African Sahel has become wetter during the last 30 years, but dry spells are shorter and more frequent *Clim. Res.* **75** 155–62 Online: https://www.int-res.com/abstracts/cr/v75/n2/p155-162/

Brown O and Crawford A 2008 Climate change: A new threat to stability in West Africa? Evidence from Ghana and Burkina Faso *African Secur. Rev.* **17** 39–57

Budyko M I 1977 Climatic changes *American Geophysical Union* (Washington, D.C) p 261

Chen L, Chen X, Cheng L, Zhou P and Liu Z 2019 Compound hot droughts over China: Identification, risk patterns and variations *Atmos. Res.* **227** 210–9 Online: https://doi.org/10.1016/j.atmosres.2019.05.009

Crutzen P J 2006 Albedo enhancement by stratospheric sulfur injections: A contribution to resolve a policy dilemma? *Clim. Change* **77** 211–20

Da-Allada C Y, Baloïtcha E, Alamou E A, Awo F M, Bonou F, Pomalegni Y, Biao E I, Obada E, Zandagba J E, Tilmes S and Irvine P J 2020 Changes in West African Summer Monsoon Precipitation Under Stratospheric Aerosol Geoengineering *Earth's Futur.* **8** 1–13

Diba I, Camara M, Sarr A B and Basse J 2021 Caractérisation des extrêmes composés de précipitation et de température au Sénégal : climat présent et futur Résumé *Afrique Sci.* **18** 12–30

Diedhiou A, Bichet A, Wartenburger R, Seneviratne S I, Rowell D P, Sylla M B, Diallo I, Todzo S, Touré N E, Camara M, Ngatchah B N, Kane N A, Tall L and Affholder F 2018 Changes in climate extremes over West and Central Africa at 1.5 °c and 2 °c global warming *Environ. Res. Lett.* **13**

Drakes O and Tate E 2022 Social vulnerability in a multi-hazard context: a systematic review *Environ. Res. Lett.* **17** 033001

Falchetta G, Gernaat D E H J, Hunt J and Sterl S 2019 Hydropower dependency and climate change in sub-Saharan Africa: A nexus framework and evidence-based review *J. Clean.*

Prod. **231** 1399–417 Online: https://doi.org/10.1016/j.jclepro.2019.05.263

Feng S, Wu X, Hao Z, Hao Y, Zhang X and Hao F 2020 A database for characteristics and variations of global compound dry and hot events *Weather Clim. Extrem.* **30** 100299 Online: https://doi.org/10.1016/j.wace.2020.100299

Field C B, Barros V, Stocker T F, Dahe Q, Dokken D J, Ebi K L, Mastrandrea M D, Pauline K J M, Plattner G-K, Allen S K, Tignor M and Midgley P M 2011 *Special Report of the Intergovernmental Panel on Climate Change Edited*

Giorgi F and Francisco R 2000 Uncertainties in regional climate change prediction: A regional analysis of ensemble simulations with the HADCM2 coupled AOGCM *Clim. Dyn.* **16** 169–82

Hales S, Edwards S J and Kovats R S 2003 Impacts on health of climate extremes *Climate change and human health: Risks and responses* pp 79–102 Online: https://www.who.int/globalchange/publications/climatechangechap5.pdf

Hao Z, Hao F, Singh V P and Zhang X 2018a Changes in the severity of compound drought and hot extremes over global land areas *Environ. Res. Lett.* **13**

Hao Z, Singh V P and Hao F 2018b Compound extremes in hydroclimatology: A review *Water (Switzerland)* **10** 16–21

He X and Sheffield J 2020 Lagged Compound Occurrence of Droughts and Pluvials Globally Over the Past Seven Decades *Geophys. Res. Lett.* **47**

Janssen A 2005 Resampling student's t-type statistics *Ann. Inst. Stat. Math.* **57** 507–29

Karami K, Tilmes S, Muri H and Mousavi S V. 2020 Storm Track Changes in the Middle East and North Africa Under Stratospheric Aerosol Geoengineering *Geophys. Res. Lett.* **47**

Klein Tank A M G, Zwiers F W and Zhang X 2009 *Guidelines on Extremes Guidelines on Analysis of extremes in a changing climate in support of informed decisions* Online: File Attachment

Kravitz B, Robock A, Boucher O, Schmidt H, Taylor K E, Stenchikov G and Schulz M 2011 The Geoengineering Model Intercomparison Project (GeoMIP) *Atmos. Sci. Lett.* **12** 162–7

Leonard M, Westra S, Phatak A, Lambert M, van den Hurk B, Mcinnes K, Risbey J, Schuster S, Jakob D and Stafford-Smith M 2014 A compound event framework for understanding extreme impacts *Wiley Interdiscip. Rev. Clim. Chang.* **5** 113–28

Lu Y, Hu H, Li C and Tian F 2018 Increasing compound events of extreme hot and dry days during growing seasons of wheat and maize in China *Sci. Rep.* **8** 1–8 Online: http://dx.doi.org/10.1038/s41598-018-34215-y

Lydersen S 2015 Statistical review: Frequently given comments *Ann. Rheum. Dis.* **74** 323–5

Niang I, Ruppel O C, Abdrabo M A, Essel A, Lennard C, Padgham J and Urquhart P 2014 Climate Change 2014: Impacts, Adaptation, and Vulnerability. Part B: Regional Aspects. Contribution of Working Group II to the Fifth Assessment Report of the Intergovernmental Panel on Climate Change *Africa* ed Pauline Dube (Botswana) and N L (USA) (Cambridge University Press, Cambridge, United Kingdom and New York, NY, USA) pp 1199–265

Nicholson S, Jinnah S and Gillespie A 2018 Solar radiation management: a proposal for immediate polycentric governance *Clim. Policy* **18** 322–34 Online: https://doi.org/10.1080/14693062.2017.1400944

Obahoundje S, N'guessan-Bi V H, Diedhiou A, Kravitz B and Moore J C 2022 Influence of stratospheric aerosol geoengineering on temperature mean and precipitation extremes indices in Africa *Int. J. Clim. Chang. Strateg. Manag.*

Odoulami R C, New M, Wolski P, Guillemet G, Pinto I, Lennard C, Muri H and Tilmes S 2020 Stratospheric Aerosol Geoengineering could lower future risk of "Day Zero" level droughts in Cape Town *Environ. Res. Lett.* **15**

Pinto I, Jack C, Lennard C, Tilmes S and Odoulami R C 2020 Africa's Climate Response to

Solar Radiation Management With Stratospheric Aerosol *Geophys. Res. Lett.* **47** 1–10
Rabitz F 2018 Governing the termination problem in solar radiation management *Env. Polit.* **00** 1–21 Online: https://doi.org/10.1080/09644016.2018.1519879
Rahm D 2018 GEOENGINEERING CLIMATE CHANGE SOLUTIONS : PUBLIC POLICY ISSUES FOR NATIONAL AND GLOBAL GOVERNANCE *Humanit. andSocial Sci. Rev.* **08** 139–48
Robock A 2000 Ic Eruptions *Rev. Geophys.* **38** 191–219
Sedlmeier K, Feldmann H and Schädler G 2018 Compound summer temperature and precipitation extremes over central Europe *Theor. Appl. Climatol.* **131** 1493–501
Seneviratne S I, Nicholls N, Easterling D, Goodess C M, Kanae S, Kossin J, Luo Y, Marengo J, Mc Innes K, Rahimi M, Reichstein M, Sorteberg A, Vera C, Zhang X, Rusticucci M, Semenov V, Alexander L V., Allen S, Benito G, Cavazos T, Clague J, Conway D, Della-Marta P M, Gerber M, Gong S, Goswami B N, Hemer M, Huggel C, Van den Hurk B, Kharin V V., Kitoh A, Klein Tank A M G, Li G, Mason S, Mc Guire W, Van Oldenborgh G J, Orlowsky B, Smith S, Thiaw W, Velegrakis A, Yiou P, Zhang T, Zhou T and Zwiers F W 2012 Changes in climate extremes and their impacts on the natural physical environment *Managing the Risks of Extreme Events and Disasters to Advance Climate Change Adaptation: Special Report of the Intergovernmental Panel on Climate Change* vol 9781107025, ed M T [Field, C.B., V. Barros, T.F. Stocker, D. Qin, D.J. Dokken, K.L. Ebi, M.D. Mastrandrea, K.J. Mach, G.-K. Plattner, S.K. Allen and and P M M (eds.)]. (Cambridge University Press, Cambridge, UK, and New York, NY, USA) pp 109–230
Tavakol A, Rahmani V and Harrington J 2020 Probability of compound climate extremes in a changing climate: A copula-based study of hot, dry, and windy events in the central United States *Environ. Res. Lett.* **15**
Tencer B, Bettolli M L and Rusticucci M 2016 Compound temperature and precipitation

extreme events in southern South America: Associated atmospheric circulation, and simulations by a multi-RCM ensemble *Clim. Res.* **68** 183–99

Uğuz H, Goyal A, Meenpal T, Selesnick I W, Baraniuk R G, Kingsbury N G, Haiter Lenin A, Mary Vasanthi S, Jayasree T, Adam M, Ng E Y K, Oh S L, Heng M L, Hagiwara Y, Tan J H, Tong J W K, Acharya U R, Cappiello G, Das S, Mazomenos E B, Maharatna K, Koulaouzidis G, Morgan J, Puddu P E, Goda M A, Hajas P, Clifford G D, Liu C, Moody B, Springer D, Silva I, Li Q, Mark R G, Kristomo D, Hidayat R, Soesanti I, Kusjani A, Grzegorczyk I, Solinski M, Lepek M, Perka A, Rosinski J, Rymko J, Stepien K, Gieraltowski J, Ghaffari A, Homaeinezhad M R, Khazraee M, Daevaeiha M M, Xu J, Durand L G, Pibarot P, Randhawa S K, Singh M, Robinson J, Xi K, Kumar R V, Ferrari A C, Au H, Titirici M-M, Parra Puerto A, Kucernak A, Fitch S D S, Garcia-Araez N, Herzig J, Bickel A, Eitan A, Intrator N, Robinson J, Xi K, Kumar R V, Ferrari A C, Au H, Titirici M-M, Parra Puerto A, Kucernak A, Fitch S D S, Garcia-Araez N, Search H, Journals C, Contact A, Iopscience M, Address I P, Rahman A M, Manuscript T A, Publishing I O P, Manuscript A, Manuscript A, By-nc-nd C C, Manuscript A, Liu C, Springer D, Clifford G D, Atul D verma, Meixiang Xiang and Y H L S Q G X J F, Kay E, Agarwal A, Gjoreski M, et al 2020 Probabilistic impacts of compound dry and hot events on global gross primary production *J. Phys. Energy* **2** 0–31

Vogel J, Paton E, Aich V and Bronstert A 2021 Increasing compound warm spells and droughts in the Mediterranean Basin *Weather Clim. Extrem.* **32** 100312 Online: https://doi.org/10.1016/j.wace.2021.100312

Wang X, Lang X and Jiang D 2022 Detectable anthropogenic influence on compound hot events over China during 1965–2014 *Environ. Res. Lett.* **17** 1–12

Watanabe S, Hajima T, Sudo K, Nagashima T, Takemura T, Okajima H, Nozawa T, Kawase H, Abe M, Yokohata T, Ise T, Sato H, Kato E, Takata K, Emori S and Kawamiya M 2011 MIROC-ESM 2010: Model description and basic results of CMIP5-20c3m experiments *Geosci. Model Dev.* **4** 845–72

Weber T, Bowyer P, Rechid D, Pfeifer S, Raffaele F, Remedio A R, Teichmann C and Jacob D 2020 Analysis of Compound Climate Extremes and Exposed Population in Africa Under Two Different Emission Scenarios *Earth's Futur.* **8** 1–19

Wu X, Hao Z, Tang Q, Singh V P, Zhang X and Hao F 2020 Projected increase in compound dry and hot events over global land areas *Int. J. Climatol.* **41** 393–403

Yu R and Zhai P 2020 More frequent and widespread persistent compound drought and heat event observed in China *Sci. Rep.* **10** 1–7 Online: https://doi.org/10.1038/s41598-020-71312-3

Zhan W, He X, Sheffield J and Wood E F 2020 Projected Seasonal Changes in Large-Scale Global Precipitation and Temperature Extremes Based on the CMIP5 Ensemble *J. Clim.* **33** 5651–71

Zhang J, Gao Y, Luo K, Leung L R, Zhang Y, Wang K and Fan J 2018 Impacts of compound extreme weather events on ozone in the present and future *Atmos. Chem. Phys. Discuss.* 1–32

Zhang Y, Hao Z, Zhang X and Hao F 2022 Anthropogenically forced increases in compound dry and hot events at the global and continental scales *Environ. Res. Lett.* **17** 024018

Zhou P and Liu Z 2018 Likelihood of concurrent climate extremes and variations over China *Environ. Res. Lett.* **13** 94023 Online: http://dx.doi.org/10.1088/1748-9326/aade9e

Zscheischler J, Martius O, Westra S, Bevacqua E, Raymond C, Horton R M, van den Hurk B, AghaKouchak A, Jézéquel A, Mahecha M D, Maraun D, Ramos A M, Ridder N N, Thiery W and Vignotto E 2020 A typology of compound weather and climate events *Nat. Rev. Earth Environ.* **1** 333–47

Zscheischler J, Westra S, Van Den Hurk B J J M, Seneviratne S I, Ward P J, Pitman A, Aghakouchak A, Bresch D N, Leonard M, Wahl T and Zhang X 2018 Future climate risk from compound events *Nat. Clim. Chang.* **8** 469–77 Online:

http://dx.doi.org/10.1038/s41558-018-0156-3

Graphical abstract

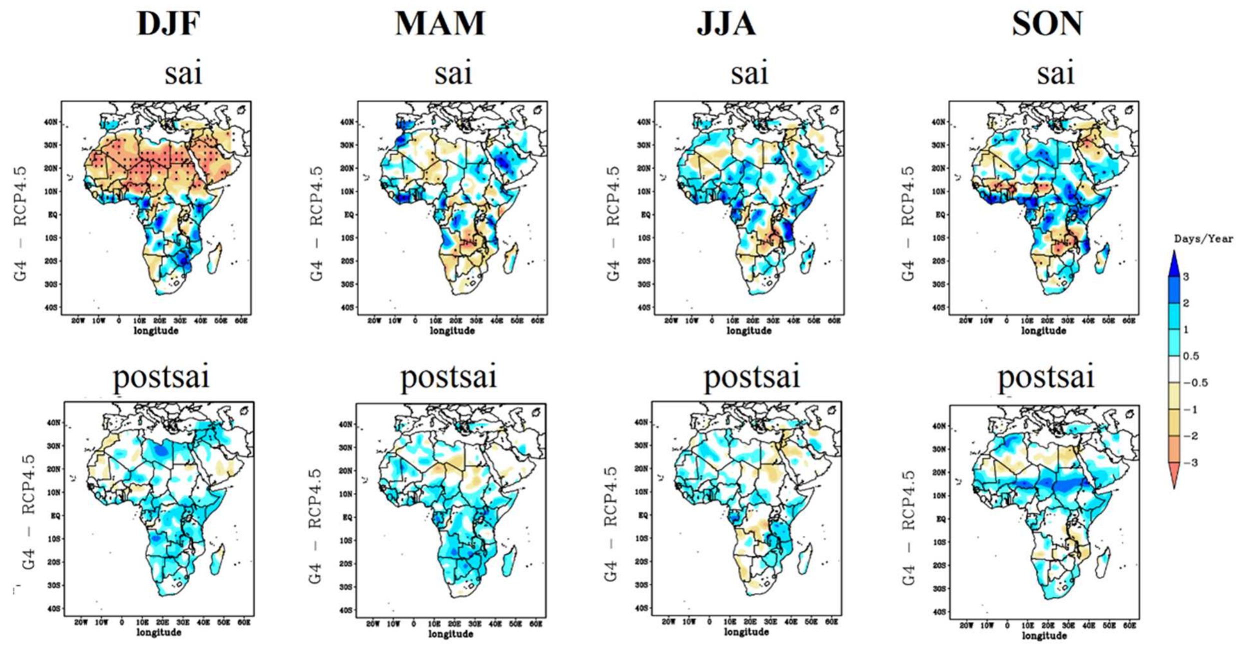

Figure : Mean changes in warm-dry compound extreme events in different seasons: DJF (first column), MAM (second column), JJA (third column) and SON (fourth column). NB: The black dots on the maps delimit areas with significant changes at the 95% confidence level; the SAI period refers to 2050-2069 and the PostSAI period refers to 2070-2089. The first row of figures compares the G4 to RCP4.5 experiments during the injection period SAI. The second row of figures compares the changes between G4 and RCP4.5 during the post-injection (PostSAI) period.